Vertical Motion of Neutrally Buoyant Floats

LOUIS GOODMAN AND EDWARD R. LEVINE

Naval Underwater Systems Center, Newport, Rhode Island

(Manuscript received 1 July 1988, in final form 10 July 1989)

ABSTRACT

The vertical motion of a neutrally buoyant float is determined from the solution to the nonlinear forced harmonic oscillator equation originally set forth by Voorhis. Float response to forced vertical oscillations is characterized by the response ratio, $r = \xi_r/\xi_w$, where ξ_r is the vertical displacement of an isopycnal relative to the float, and ξ_w is the vertical displacement of an isopycnal relative to its initial equilibrium position. For isopycnal displacements with frequencies much less than the resonant frequency of the float, the float can be considered to be in near dynamic equilibrium with the forcing, and r is a function of the relative compressibility between the float and seawater, $s = \gamma_f/\gamma_w$, and the normalized buoyancy frequency $\mathcal{N} = N/\Omega$, where Ω is a characteristic float frequency defined by $\Omega^2 = g\gamma_w[1 - (\alpha_f\alpha_w^{-1})]^{-1}$, where α_f, α_w are the coefficients of thermal expansion of the float and water, respectively. For the near dynamic equilibrium case, data obtained from a float deployment in a Gulf Stream meander result in an observed r value close to the predicted value. For the case of float response to an isopycnal displacement of frequency near the resonant frequency of the float, vertical motion depends on drag, in addition to the material properties of the float and seawater. The bandwidth over which resonance can occur is parametrized by the 'Q' factor, the inverse of the normalized bandwidth, which for cylindrical floats is predicted to be greater than 1, indicating sharp resonance. From a float deployment in the Gulf Stream region it was estimated that $Q \approx 5$. For this case, the spectrum of float temperature, which was used as an indicator of the relative response between the float and a displaced isopycnal, and the spectrum of the float pressure, used as an indicator of float displacement, did scale according to that predicted by the condition of near equilibrium response, up to of order the resonant frequency of the float.

1. Introduction

Neutrally buoyant floats are becoming more important as tools in physical oceanography for water parcel tagging over a wide variety of scales of motion. Studies of mesoscale circulation have been conducted using ship tracked Swallow floats (Swallow 1955; Gascard and Clark 1983; Levine et al. 1986), acoustic telemetering SOFAR floats which transmit to moored (Rossby et al. 1975; Price and Rossby 1982) or icebound (Manley et al. 1989) listening stations, and acoustic receiving RAFOS floats (Rossby et al. 1985b, 1986). Studies of internal waves with freely drifting floats have been carried out by Pochapsky (1963) using Swallow floats, and by Voorhis (1968) using vane instrumented neutrally buoyant floats to measure vertical velocity. Cairns (1975) measured internal waves using a float capable of freely drifting as well as oscillating vertically by means of a buoyancy control device. More recent advances in float design include the Richardson number float (Williams et al. 1987), the bellows-equipped oscillating float (Davis, personal communication), and the oscillating RAFOS float (Rossby, personal communication).

Corresponding author address: Dr. Louis Goodman, Naval Underwater Systems Center, Newport, RI 02841.

Freely drifting floats are typically deployed as near-isobaric followers of water parcels, while floats which vertically oscillate using buoyancy control are used to obtain the vertical displacement of isotherms. Recent efforts have been made towards the development of more isopycnal-like floats by matching the compressibility of the float to that of seawater by means of a compressee (Rossby et al. 1985a). Near isopycnal Swallow floats were successfully deployed in a Gulf Stream meander (Levine et al. 1986), and near isopycnal RAFOS floats have also been tracked by Rossby et al. (1985a) for larger scale Gulf Stream and other experiments. Hitchcock et al. (1989) deployed near isopycnal floats equipped with fluorometers in the Gulf Stream and elsewhere to examine the upper ocean chlorophyll distribution.

Float response to vertical motion can be divided into three regimes (Fig. 1): 1) settling, 2) equilibrium, and 3) near resonance. The neutrally buoyant float has near perfect response to horizontal motion and thus only vertical response to isopycnal displacement forcing needs to be considered. In addition, the effects of vertical velocity shear can be ignored for stable configurations, i.e., the center of gravity located well below the center of buoyancy (Voorhis 1971), and tipping effects are negligible for floats with body types and sizes considered in this paper.

Unauthenticated | Downloaded 11/29/23 05:35 AM UTC

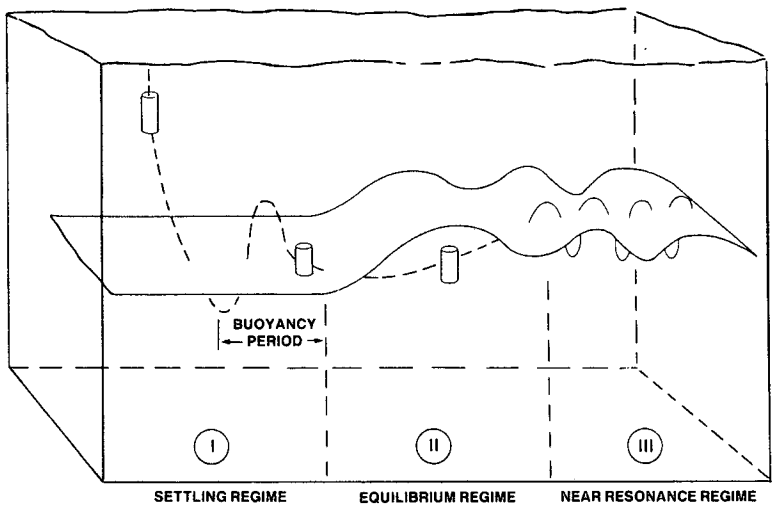

FIG. 1. Float response regimes.

In Regime 1, settling is the result of a near balance between the weight of the float in water and its drag. For most realistic drag values, the float overshoots and then oscillates at its resonant frequency about its equilibrium position. In Regime 2, isopycnal displacements occur over sufficiently long periods that the float can be considered in dynamic equilibrium, even though it is undergoing vertical displacement. Regime 3 refers to float vertical displacement near the float resonant frequency and is a function of the specific form of the drag, and, hence, body size and shape.

The dynamic response of a neutrally buoyant freely drifting float to vertical water motion has been examined by a number of authors. In the laboratory, Larsen (1969) studied response in Regime 3 for a salt stratified fluid with very large buoyancy frequencies, 383 cyc h^{-1} and 636 cyc h^{-1}. For these examples, the drag is dominated by float-induced internal waves. Laboratory results were in very good agreement with theoretical curves describing float response due to the generation of internal waves.

A comprehensive treatment of the problem of the equilibrium response of floats to vertical motion was carried out by Voorhis (1971), who considered both spherical and cylindrical shaped bodies. He used a quadratic drag law for large Reynolds number cases and a linear drag law for small Reynolds number cases, including in the latter results of Larsen (1969) for internal wave-induced drag. Voorhis shows that internal wave-induced drag and inertia effects are a strong function of body shape, and can be neglected for streamlined bodies with large length to width ratios.

A combined theoretical and observational study of the response of a spherical "Snodgrass capsule" deployed in Lake Tahoe was carried out by Cairns et al. (1979). This instrument had previously been used by Cairns (1975) and Cairns and Williams (1976) for open-ocean internal wave studies. Cairns et al. (1979) modeled the float as a nonlinear harmonic oscillator with a quadratic drag law. In their observations they found that during deployment large air bubbles were trapped to the struts of the instrument. Subsequently, Rossby et al. (1985a) found that pressurization of floats prior to laboratory ballasting greatly reduces depth overshooting in situ. Taking into account the effect of air bubbles on buoyancy, the theory of Cairns et al. (1979) compared very well with data for the descent phase of Regime 1. Their float overshot the equilibrium position with approximately the predicted amplitude, as expected. However, it did not oscillate about the equilibrium position behaving instead in an exponentially damped manner that could not be explained by any realistic increased drag.

Cairns et al. (1979) also obtained a unique set of internal wave displacement data from their float pressure sensor. The spectrum of vertically induced float displacement (their Fig. 9), has a dynamic range up to the float resonant frequency, almost a decade and a half beyond where rapid drop off of the spectrum occurs. The overall variance of float displacement is estimated to be 1 cm^2 from calculations based on (3.3), which suggests that the float response, nearly isobaric, is approximately 0.2% of the internal wave vertical displacements, with the internal wave displacement variance of order 25 m^2. The spectrum itself is red and has a power law of order -2, up to a frequency characteristic of the shallow buoyancy frequency maximum, which is itself larger than the local buoyancy frequency, and is suggestive of the presence of evanescent internal waves. This result is a good example of the potential of using a freely drifting float to obtain the full dynamic range of internal waves in their intrinsic frequency domain, provided that the response of the float is known.

Unauthenticated | Downloaded 11/29/23 05:35 AM UTC

2. Float vertical displacement equation

The fundamental float vertical response equation is derived in a coordinate system in which z is the vertical position taken as positive upwards. For $t \leq 0$, we assume that the water is at rest with the float in equilibrium at depth Z_0 where $\rho_f(0) = \rho_w(Z_0, 0) = \rho_0$, with $\rho_w(Z, t)$ and $\rho_f(t)$ the water and float densities, respectively, and ρ_0 the density of seawater at the initial equilibrium depth. Let $Z_w(t)$ be the vertical position of the isopycnal in which the float is at equilibrium at $t = 0$ with $Z_f(0) = Z_w(0) = Z_0$, where $Z_f(t)$ is the vertical position of the float. The equation of motion for a float in water is

$$m(d^2Z_f/dt^2) = F, \tag{2.1}$$

where m is the mass of the float, and the quantity F is the total body force on the float which can be written as the sum

$$F = F_0 + F_i + F_d, \tag{2.2}$$

where $F_0 + F_i$ is the net body force produced by the pressure field of the surrounding water, with F_0 the body force in the absence of the flow distortion effect of the body and F_i the additional body force due to the actual pressure field surrounding the body in a stratified fluid, and F_d is the total drag force, including skin drag, form drag, and wave drag associated with radiated internal waves.

Using Gauss' law with the definition of F_0 it follows that

$$\begin{aligned} F_0 &= \int p d\mathbf{s} - mg = -V dp/dz - mg \\ &= Vg\{[\rho_w(Z_f) - \rho_f(Z_f)] + [\rho_w(Z_f)/g]du/dt\} \\ &\approx Vg\{[\rho_w(Z_f) - \rho_f(Z_f)] + [\rho_w(Z_f)/g]d^2Z_w/dt^2\}, \end{aligned} \tag{2.3}$$

where the vertical velocity of the water, w, at the depth Z_f is approximated by

$$w(Z_f, t) \approx w(Z_w, t) = dZ_w/dt, \tag{2.4}$$

$d\mathbf{s}$ is the differential vector area, and V the volume of the float.

From Voorhis (1971) it can be shown that F_i can be expressed in the form

$$F_i = V\rho_w \delta d^2\xi_r/dt^2, \tag{2.5}$$

where $\xi_r = Z_w - Z_f$ is the relative displacement between the equilibrium isopycnal and the float, and we have again used (2.4). The quantity δ is the normalized added mass. [Note that (2.5) is often expressed in the frequency domain as a product, with δ, in general, frequency dependent. This frequency dependence can arise from the generation of internal waves by the float and also by viscous effects. For the size and shape floats employed in this work this effect is negligible.]

The drag term F_d is taken to have the functional form $F_d(\mathrm{Re})$, where Re is the Reynolds number. The explicit form of F_d as a function of body shape will be discussed in section 4.

Substitution of Eqs. (2.2), (2.3) and (2.5) into (2.1), using the Boussinesq approximation in replacing ρ_w and ρ_f by ρ_0, except where multiplied by g, the density at the equilibrium depth of the float, yields

$$(1 + \delta)\rho_0 d^2\xi_r/dt^2 = -(\rho_w - \rho_f)g - F_d V^{-1}. \tag{2.6}$$

The change in density of a water parcel surrounding the float in going from the initial equilibrium position, Z_0, to Z_f, can be considered as the sum of two terms, a potential density change, $\delta\rho_{\mathrm{pot}}$, and an adiabatic change, $\delta\rho_a$, i.e.

$$\delta\rho_w = \rho_w(Z_f) - \rho_0 = \delta\rho_{\mathrm{pot}} + \delta\rho_a, \tag{2.7}$$

where

$$\delta\rho_{\mathrm{pot}} = (\rho_0 N^2 g^{-1})\xi_r, \tag{2.8a}$$

with N, the buoyancy frequency, assumed constant over the vertical distance, ξ_r. The adiabatic change in the water density surrounding the float is given by

$$\delta\rho_a = -(\rho_0)^2 g\gamma_w \xi_f, \tag{2.8b}$$

where

$$\xi_f = Z_f - Z_0$$

and γ_w is the compressibility of seawater, defined by

$$\gamma_w = (1/\rho_w)(\partial\rho_w/\partial P)_a \approx (1/\rho_0)(\partial\rho_w/\partial P)_a.$$

The subscript a refers to an adiabatic (constant entropy) change. For the calculation of the change of float density with vertical displacement, note that for typical float materials the thermal conductivity is sufficiently large that the float will equilibrate to the surrounding water temperature on a time scale much shorter than its own characteristic oscillation time (Voorhis 1971). This allows the change in float density to be written as

$$\delta\rho_f = \rho_f(Z_f, t) - \rho_0 = \delta\rho_T + \delta\rho_P, \tag{2.9}$$

i.e., the change in float density due to its change in temperature, $\delta\rho_T$, and that due to its change in pressure, $\delta\rho_P$. These terms can be expressed as

$$\begin{aligned} \delta\rho_T &= -\rho_0\alpha_f\delta T_f \\ &= \rho_0\alpha_f\{(dT/dz)\xi_r + (d\theta/dz)\xi_w\} \end{aligned} \tag{2.10a}$$

$$\delta\rho_P = -(\rho_0)^2 g\gamma_f\xi_f, \tag{2.10b}$$

where the first term of (2.10a) represents the effect of the change in temperature which the float senses between the water mass at Z_0 and Z_f corrected by the second term, the adiabatic change in temperature due to the water mass displacement $\xi_w = Z_w - Z_0$; dT/dz and $d\theta/dz$ are the temperature gradient and the adi-

Unauthenticated | Downloaded 11/29/23 05:35 AM UTC

abatic temperature gradient, assumed constant over the vertical distances ξ_r and ξ_w, respectively. The coefficients of thermal expansion and compressibility of the float are defined by

$$\alpha_f = -(\rho_f)^{-1}(\partial\rho_f/\partial T)_P,$$

$$\gamma_f = (\rho_f)^{-1}(\partial\rho_f/\partial P)_T,$$

respectively. Substitution of (2.7) through (2.10) into (2.6) with some straightforward algebra, yields

$$(d^2\xi_r/dt^2) + \sigma d\xi_r/dt + (\omega_0)^2\xi_r = (\omega_1)^2\xi_w, \quad (2.11)$$

where

$$\sigma = F_d[(1+\delta)\rho_0 V d\xi_r/dt]^{-1} = 0.5C_D l^{-1}|d\xi_r/dt| \quad (2.12)$$

and C_D is the drag coefficient which is a function of float Reynolds number, Re,

$$C_D = C_D(\mathrm{Re}),$$

$$l = V(1+\delta)[A]^{-1},$$

where A is the effective cross-sectional area of the float, and

$$\mathrm{Re} = Ulv^{-1}.$$

The parameters U, I are the characteristic float velocity relative to the water, and the length, and ν is the kinematic viscosity of seawater. The frequencies, ω_0, ω_1, are given by

$$(1+\delta)(\omega_0)^2 = N^2 + \rho_0 g^2(\gamma_w - \gamma_f) - g\alpha_f(dT/dz) \quad (2.13)$$

$$(1+\delta)(\omega_1)^2 = \rho_0 g^2(\gamma_w - \gamma_f) + g\alpha_f(d\theta/dz). \quad (2.14)$$

The frequency ω_0 represents the natural frequency of oscillation of the float from the buoyancy force per unit mass between the float and the water surrounding the float with the frequency ω_1 associated with adiabatic changes in the buoyancy force per unit mass. The case of $dT/dz = 0$ along with $d\theta/dz \approx 0$ results in $\omega_0 = \omega_1$ and the asymptotic solution $\xi_r = \xi_w$, or $\xi_f = 0$. Thus, the difference $(\omega_0^2 - \omega_1^2)$ determines the effectiveness of the isopycnal displacement forcing in moving the float vertically. Note that (2.11) is essentially identical to Eq. (61) of Voorhis (1971).

3. Near equilibrium regime

For a water parcel displacement time scale τ such that

$$\tau \gg (\omega_0)^{-1} \quad (3.1a)$$

$$\tau \gg \sigma\omega_0^{-2}, \quad (3.1b)$$

the first two terms on the left hand side of (2.11) can be neglected and we obtain the equilibrium limit

$$\xi_r = (\omega_1/\omega_0)^2\xi_w. \quad (3.1c)$$

We define the response ratio as

$$r = \xi_r/\xi_w.$$

From (3.1c), using (2.13) and (2.14), we can write

$$r = [1 - s + \alpha_f(d\theta/dz)/(\rho_0 g^2\gamma_w)]/$$
$$[1 - s + (N^2 - \alpha_f dT/dz)/(\rho_0 g^2\gamma_w)]$$
$$\approx [1-s]/[1 - s + N^2/(\rho_0 g^2\gamma_w) - (\alpha_f dT/dz)/(\rho_0 g^2\gamma_w)], \quad (3.2)$$

where s is the relative compressibility of the float defined as

$$S = \gamma_f/\gamma_w.$$

Since for realistic float values $\alpha_f|d\theta/dz|/(\rho_0 g^2\gamma_w) \leq 10^{-2}$, this term has been dropped in (3.2). (Note that in subsequent discussions on the behavior of r about $s = 1$ the presence of the adiabatic temperature gradient term results in a small shift, of order 10^{-2}, from $s = 1$ in the location of the $r = 0$ point, and does not change significantly, i.e., again to of order 10^{-2}, the behavior of r about $s = 1$.) For the case where the salinity gradient does not make a significant contribution to N, (3.2) can be written

$$r \approx [1 - s]/[1 - s + \mathcal{N}^2], \quad (3.3)$$

where

$$\mathcal{N} = N/\Omega,$$

$$\Omega^2 = \rho_0 g^2\gamma_w/[1 - (\alpha_f\alpha_w^{-1})], \quad (3.4)$$

where

$$\alpha_w = -(\rho_f)^{-1}(\partial\rho_w/\partial T)_P.$$

Here Ω is a characteristic frequency which is related to the float resonant frequency by

$$(1+\delta)\omega_0^2 = [1 - (\alpha_f\alpha_w^{-1})][N^2 + \Omega^2(1-s)] \quad (3.5)$$

from (2.11). For the case where the coefficient of thermal expansion of the float is much less than that of seawater,

$$\alpha_f\alpha_w^{-1} \ll 1,$$

$$\Omega = gc^{-1} \approx 3.8 \text{ cyc h}^{-1},$$

where c is the speed of sound in seawater, a quantity which varies by $\leq 5\%$ over the world's oceans. Note that for the case of $\mathcal{N}^2 \ll 1 - s$ using

$$r = \xi_r/\xi_w = (\xi_w - \xi_f)/\xi_w = 1 - (\xi_f/\xi_w)$$

from (3.3) it follows that

$$\xi_f/\xi_w \approx \mathcal{N}^2/(1-s) \ll 1, \quad (3.6)$$

Unauthenticated | Downloaded 11/29/23 05:35 AM UTC

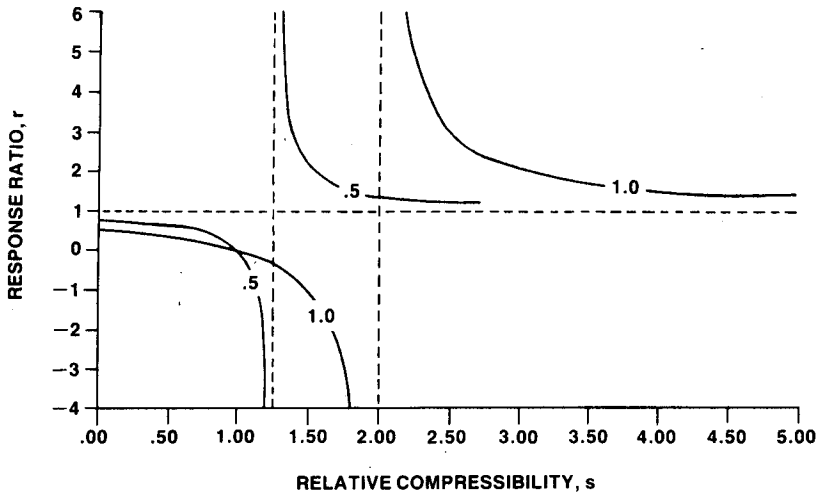

FIG. 2a. Low-frequency response ratio, $r = \xi_r/\xi_w$, as a function of relative compressibility (3.3) over the range $0 < s < 5$, for $\mathcal{N} = 0.50$ and 1.00, $\mathcal{N}$ the normalized buoyancy frequency, $\mathcal{N} = N/\Omega$, Ω given by (3.4). The values $r = 0$, 1 correspond to the perfectly isopycnal and isobaric cases, respectively.

a result which may be applicable to the deep-ocean case.

In Fig. 2a we show a plot of r versus s for $\mathcal{N} = 0.5$ and 1.0 from (3.3). When $\xi_r = 0$, $r = 0$, the perfectly isopycnal case, the float has the same vertical displacement as the isopycnal displacement, $\xi_f = Z_f - Z_0$. When $\xi_f = 0$, $r = 1$, we have the perfectly isobaric case. This figure presents the response ratio r for the range of s values $0 < s < 5$, which, for the above values of $\mathcal{N}$, encompasses both the stable case, defined by $(\omega_0)^2 > 0$, i.e., restoring force opposite in sign to the relative displacement, ξ_r; and the unstable case, defined by $(\omega_0)^2 < 0$, i.e., producing a force with the same sign as the relative displacement, ξ_r. This stability criteria can be seen from (3.5) which yields,

$$(1 + \delta)(\omega_0/\Omega)^2 = [1 - (\alpha_f/\alpha_w)][\mathcal{N}^2 + (1 - s)], \tag{3.7a}$$

or, equivalently, using (3.3)

$$(1 + \delta)\omega_0^2 = [1 - (\alpha_f/\alpha_w)]N^2(1 - r)^{-1}. \tag{3.7b}$$

Note that the second factor on the right hand side of (3.7a) appears in the denominator of r, in (3.3). Thus the neutral stability criteria

$$\omega_0 = 0$$

corresponding to

$$s = 1 + \mathcal{N}^2$$

are the infinite asymptotes of r, shown as vertical lines in Fig. 2a, and represent the points at which the total density gradient of the float is greater than that of the surrounding seawater. An expanded version of this figure for the range $0.0 < s < 1.20$ is shown in Fig. 2b, to emphasize the behavior of r for s near 1.

From the definition of $\mathcal{N}^2$ following (3.3) $\mathcal{N}^2 > 0$ if $\alpha_f/\alpha_w < 1$ and $\mathcal{N}^2 < 0$ if $\alpha_f/\alpha_w > 1$. If we confine ourselves to the case of $\alpha_f/\alpha_w < 1$ for $1 < s < 1 + \mathcal{N}^2$ the float remains in the stable regime, but from (3.3) results in $r < 0$, since the total density gradient of the float is less than that of seawater. If $s > 1 + \mathcal{N}^2$ the compressibility of the float has become so large that the total float density gradient is greater than that of seawater, and thus the float does not move as far vertically as the surrounding isopycnal surface. This results in $r > 0$, as noted by the positive values of r for $s > 1 + \mathcal{N}^2$ in Fig. 2a. However, r has been defined assuming equilibrium. [The acceleration term of Eq. (2.11) set equal to zero.] For the case of $s > 1 + \mathcal{N}^2$, the float is in unstable equilibrium and for any perturbation from equilibrium the float becomes unstable.

From Figs. 2a, b the slope of r about $s = 1$ for each $\mathcal{N}$ value determines how closely a float can be made to match the mechanical properties of seawater before it becomes unstable. We see that small values of $\mathcal{N}$, which correspond to the deep ocean, result in r with very large slopes about $s = 1$, and thus impose a severe constraint on the ability to produce a float with $r = 0$. This implies that it is much more difficult to achieve near isopycnal behavior for a float in deep water, where N is relatively small, than in the upper ocean pycnocline, where N is typically much larger, by adjusting the mechanical properties of floats, such as adding a compressee.

Note that $\mathcal{N}$ also contains the effect of thermal expansion on the float. For example, an aluminum float in the main thermocline in midlatitudes has α_f/α_w

Unauthenticated | Downloaded 11/29/23 05:35 AM UTC

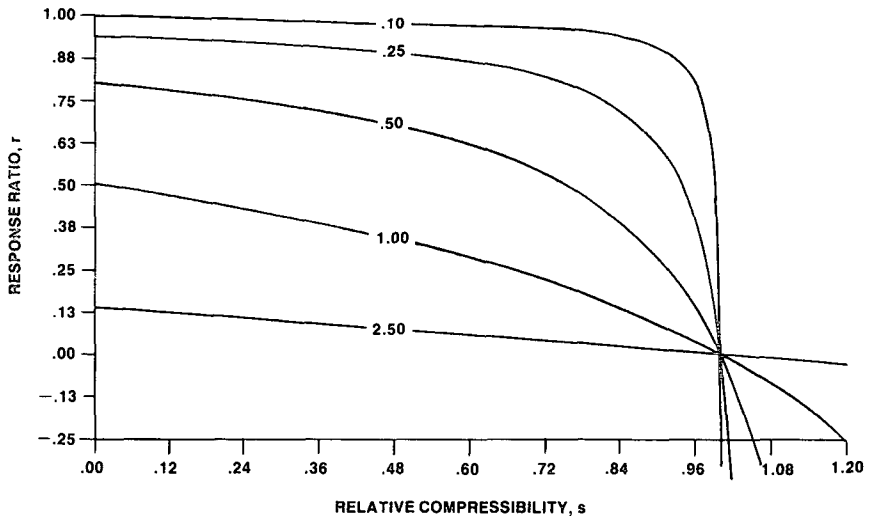

FIG. 2b. Low-frequency response ratio, $r = \xi_r/\xi_w$, as a function of relative compressibility, s, (3.3) over the range $0 < s < 1.2$ for $\mathcal{N} = 0.10$, 0.25, 0.50, 1.00, and 2.50, $\mathcal{N}$ the normalized buoyancy frequency, $\mathcal{N} = N/\Omega$, Ω given by (3.4).

≈ 0.35 which has the same effect on $\mathcal{N}$ as would occur if the thermal expansion coefficients of the float and seawater were held constant, and Ω increased by 25%. In deployments at high latitudes, particularly in the upper ocean of the Arctic, this effect can be quite significant.

Neutrally buoyant floats, such as the modified Snodgrass capsule (Cairns et al. 1975), the vertical current meter float (Voorhis 1968), and SOFAR (Rossby et al. 1975) and RAFOS (Rossby et al. 1986) floats without compressees typically have relative compressibilities $s \approx 0.5$. For a main pycnocline deployment, where $\mathcal{N} \approx 0.3$ (Fig. 2b), $r \approx 0.9$ results in a small vertical displacement of the float. By adding a compressee to the float, which has a compressibility greater than seawater (Rossby et al. 1985) the relative compressibility, s, of a float can be increased above the typical value of 0.5 and thus the float can be made to follow an isopycnal more closely. However, in the main pycnocline where SOFAR floats are typically deployed, to produce $r < 0.1$ for $\mathcal{N} \approx 0.3$ would require $s \approx 0.99$! In the upper ocean, where typically $\mathcal{N} \approx 1$, and $r \approx 0.3$ for $s = 0.5$, the addition of a compressee can result in $s \approx 0.9$ (Rossby et al. 1985), yielding $r \approx 0.1$.

Floats are typically equipped with temperature sensors which measure the temperature change due to the relative float displacement, i.e.,

$$\Delta T_F = \xi_r dT/dz = r\xi_w dT/dz. \qquad (3.8)$$

In Fig. 3 we plot $\Delta T_F/\xi_w = r dT/dZ$, the change in float temperature per meter of isopycnal displacement as a function of the relative compressibility, s. From (3.3), r decreases with increasing N and hence increasing dT/dz. Thus ΔT_F increases with increasing dT/dz but less than linearly.

A float pressure sensor can be used to measure ξ_f. Note that r can be expressed as $r = r(s, N)$ with $N^2 = g\alpha_w dT/dz$, for the case of negligible salinity effects. Thus, the combination of data from pressure and temperature sensors, for the case of $|s| \neq 1$, can be used to estimate dT/dz and ξ_w. According to Fig. 2b, the precision of a dT/dz estimate will be a strong function of s, since the r curves for different values of $\mathcal{N}$ converge near $s = 1$, resulting in poor predictions of $\mathcal{N}$ or dT/dz, but in a good prediction of ξ_w since $\xi_w = \xi_f$ at $s = 1$.

Finally, for the equilibrium regime consider the case when float thermal expansion can become an important factor in determining float response to vertical isopycnal displacement. In very high latitudes, where seawater temperature is near 0°C in the upper ocean, the seawater thermal expansion coefficient can decrease to values comparable to those of materials used in floats. In Fig. 4a, using (3.2) and including the salinity along with temperature gradient contribution to N, we show float response for the ocean environment of Fig. 4b, under pack ice in spring. Two depths are considered, at 190 m depth where the temperature gradient is a maximum (negative), and at 50 m, where N is a maximum, but a very small temperature gradient occurs and where float response is expected to be most isopycnal. Curve 1 is for a glass float at 50 m, and does exhibit the most isopycnal behavior. Curves 2 and 3 are for a glass float, $\alpha_f \approx 1 \times 10^{-5}$ °C^{-1}, and an aluminum float, $\alpha_f \approx 7.0 \times 10^{-5}$ °C^{-1} at 190 m, respectively. At this depth $\alpha_w \approx 5 \times 10^{-5}$ °C^{-1} and, thus, for aluminum, $\alpha_f > \alpha_w$. From (3.2), note that the

Unauthenticated | Downloaded 11/29/23 05:35 AM UTC

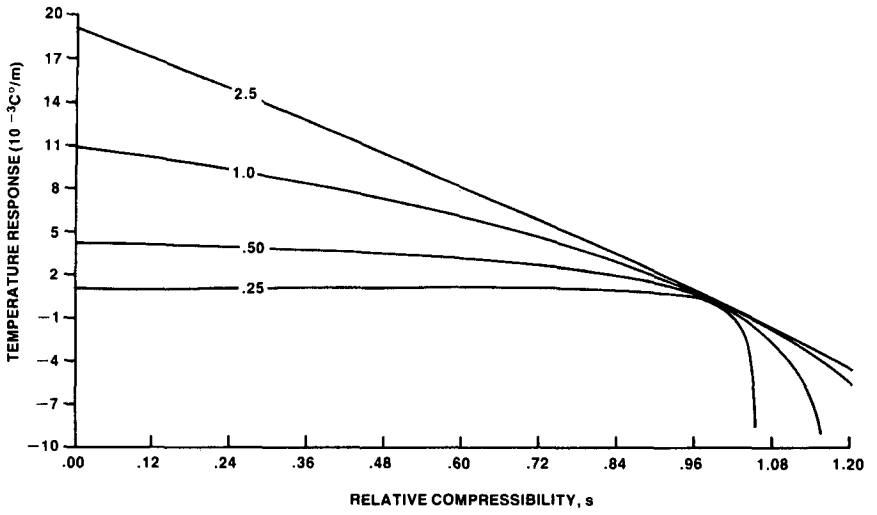

FIG. 3. Low frequency sensor temperature response, $\Delta T_F/\xi_w = rdT/dZ$, where $dT/dZ = N^2(g\alpha_w)$, as a function of $\mathcal{N} = N/\Omega$, for $\Omega = 3.76$ cyc h^{-1}.

product of α_f with the negative temperature gradient (at 190 m) has the same sign (positive) as the surrounding buoyancy frequency and thus increasing α_f in an environment with a negative temperature gradient decreases r. This can be interpreted as follows: When an isopycnal in stably stratified environment but with a negative temperature gradient rises (falls) to shallower (greater) depths the float, assumed to have a compressibility less than seawater, is not able to follow perfectly the isopycnal and would rise (fall) to some fraction, r, of the isopycnal displacement. However, the warmer (colder) water rising (falling) from depth causes a float of large thermal expansion coefficient to expand (contract) and gain (lose) buoyancy causing it to rise (fall) further and, provided the value of the float thermal expansion coefficient is not so large that the float becomes unstable, follow the displaced isopycnal more closely. This can be noted in Fig. 4a by comparing the glass float with the aluminum float at 190 m.

4. Near resonance regime

When conditions (3.1a) and (3.1b) are not valid, the float is not in equilibrium and the first two terms on the left hand side of (2.11) cannot be neglected. Resonance of the float, modeled as a harmonic oscillator described by (2.11), occurs for the frequency

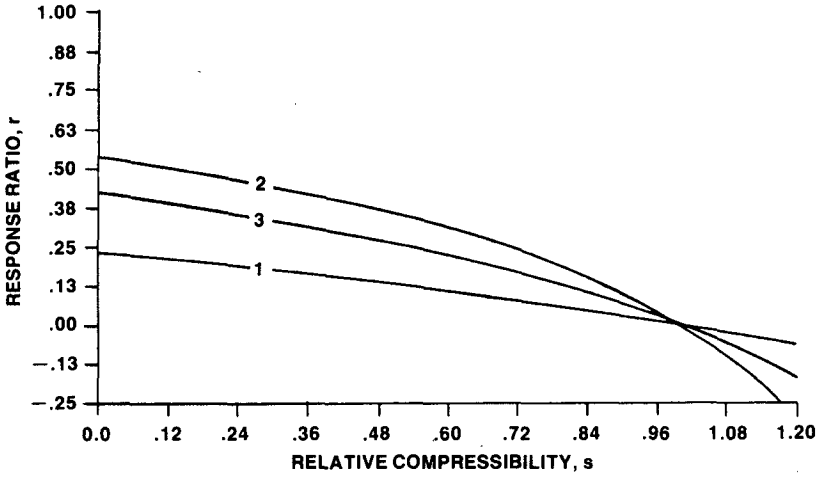

FIG. 4a. Arctic low frequency response ratio, r, as a function of relative compressibility, s, for three cases: (1) a glass float ($\alpha_f = 1.0 \times 10^{-4}$ °C^{-1}) at 50 m depth, where $N = 7.22$ cyc h^{-1}, and $\Omega = 3.95$ cyc h^{-1}; (2) a glass float at 190 m depth, where $N = 3.47$ cyc h^{-1} and $\Omega = 3.92$ cyc h^{-1}; and (3) an aluminum float ($\alpha_f = 7.0 \times 10^{-4}$ °C^{-1}) at 190 m.

Unauthenticated | Downloaded 11/29/23 05:35 AM UTC

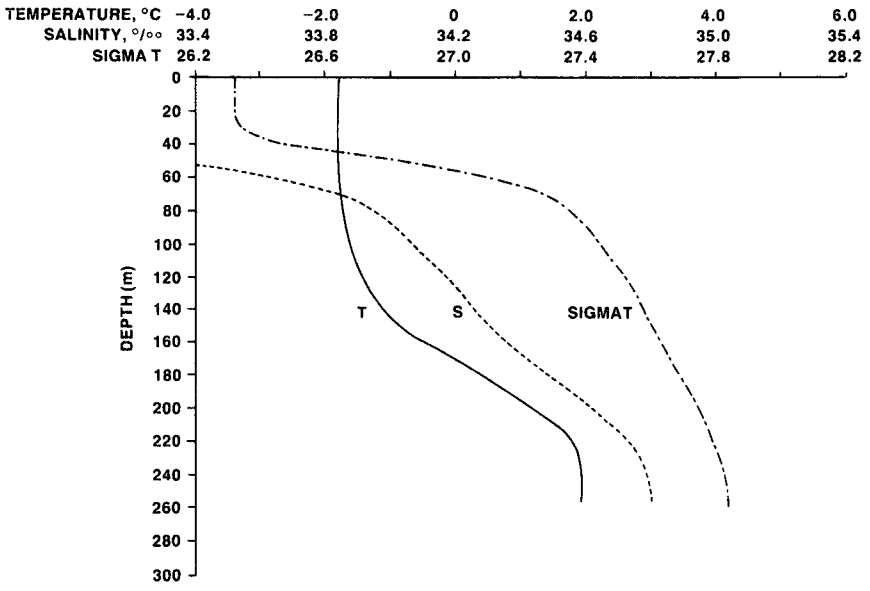

FIG. 4b. Upper-ocean temperature, salinity, and sigma t profiles obtained in Fram Strait under pack ice during the Fram III experiment (Morison and Anderson 1985).

component $\omega = \omega_0$. For the case of the Swallow or SOFAR float, long cylinders with length to radius ratio $L/R \gg 1$, Voorhis (1971) has shown that $\delta \approx 0$, and from (3.7a) it follows that

$$\omega_0^2 = \{[1 - (\alpha_f/\alpha_w)]N^2 + \Omega^2(1 - s)\}$$
$$= N^2 - (\alpha_f/\alpha_w)[N^2 - N_0^2], \quad (4.1)$$

where

$$N_0 = [(1 - s)(\alpha_f/\alpha_w)]^{1/2}\Omega \quad (4.2)$$

is the buoyancy frequency such that for $N < N_0$, $\omega_0 > N$, and we expect internal wave induced isopycnal displacements at the float resonant frequency to be small. Note that if

$$\alpha_f/\alpha_w < 1$$

when

$$N > N_0,$$

then

$$N > \omega_0 > N_0;$$

while for

$$\alpha_f/\alpha_w > 1,$$

such as the case of the aluminum float in the high latitude deployment described in section 3, when

$$N > N_0,$$

then

$$\omega_0 < N_0 < N.$$

Thus, the value of the ratio N/N_0 will determine whether there can be significant isopycnal forcing at the float resonant frequency. The ratio α_f/α_w determines the frequency range over which the isopycnal forcing can occur.

Following conventional analysis of harmonic oscillators (Kinsler et al. 1982, chapter 1), the bandwidth $\Delta\omega$ over which resonance occurs is defined as the frequency range over which the response power drops to ½ its value at resonance. The frequency $(\omega_0 - \Delta\omega/2)$ can be interpreted as the boundary in the frequency domain, between the equilibrium regime, described in section 3, and the near resonance regime. The bandwidth, $\Delta\omega$, is typically expressed in terms of the Q factor defined by

$$Q = \omega_0/(\Delta\omega), \quad (4.3)$$

where from Kinsler et al. (1982, chapter 1) $\Delta\omega = \sigma$, which upon substitution of (2.12), yields

$$\Delta\omega = \sigma = 0.5C_D l^{-1} |d\xi_r/dt|. \quad (4.4)$$

For a linear drag term in (2.12), C_D would be inversely proportional to $|d\xi_r/dt|$ and Q would be independent of the relative velocity $|d\xi_r/dt|$. In general the drag term is not linear, but if $Q \gg 1$, resonance effects are confined to the narrow bandwidth $(\omega_0 - \Delta\omega/2) < \omega < (\omega_0 + \Delta\omega/2)$.

Let b_r, b_f, and b_w be the average amplitude of the relative displacement, ξ_r, float displacement, ξ_f, and isopycnal displacement, ξ_w, over the bandwidth $(\omega_0 - \Delta\omega/2) < \omega < (\omega_0 + \Delta\omega/2)$, i.e.

$$\xi_r = b_r \exp(i\omega_0 t), \quad (4.5a)$$

$$\xi_f = b_f \exp(i\omega_0 t), \quad (4.5b)$$

$$\xi_w = b_w \exp(i\omega_0 t), \quad (4.5c)$$

Unauthenticated | Downloaded 11/29/23 05:35 AM UTC

where for $Q \gg 1$

$$(b_r)^2 \approx E_r(\omega_0)\Delta\omega \quad (4.6a)$$

$$(b_f)^2 \approx E_f(\omega_0)\Delta\omega \quad (4.6b)$$

$$(b_w)^2 \approx E_w(\omega_0)\Delta\omega, \quad (4.6c)$$

with $E_r(\omega)$, $E_f(\omega)$, $E_w(\omega)$ the relative, float, and isopycnal displacement spectra, respectively. Use of (4.3) and (4.4) in (2.11), yields a relationship for the response ratio at resonance, r_0,

$$r_0 = [E_r(\omega_0)/E_w(\omega_0)]^{1/2} = Qr, \quad (4.7)$$

where r is the equilibrium response ratio given by (3.2) or (3.3). Note that an explicit expression for Q can be obtained from (4.7) and (4.3) with (2.11) if the form of the drag coefficient is given.

For the case of SOFAR and Swallow floats, both of which are well approximated by long cylinders, the drag coefficient obeys a similar law to that of a streamlined body (Batchelor 1970, p. 335)

$$C_D = 1.33\ \mathrm{Re}^{-0.5}, \quad (4.8)$$

with a Reynolds number at resonance given by

$$\mathrm{Re} = |d\xi_r/dt| L\nu^{-1} = Lb_r\omega_0\nu^{-1},$$

where L, R are the length and radius of the cylinder, respectively. In addition, the parameter l of (2.12) is given by

$$l = VA^{-1} = 0.5R,$$

where $\delta \approx 0$ for the long cylinder case. Combining (4.8), (4.7), (4.5) and (4.2) results in

$$\Delta\omega = [3.1E_w(\omega_0)(\omega_0)^4\nu^2r^2/(R^4L^2)]^{1/5} \quad (4.9a)$$

and

$$Q = [0.3R^4L^2\omega_0/(E_w(\omega_0)\nu^2r^2)]^{1/5}. \quad (4.9b)$$

Note that as $E_w(\omega_0) \to 0$, $\Delta\omega \to 0$, $Q \to \infty$, and from (4.5) $E_r(\omega_0) \to 0$, as expected.

From (4.1) and (4.2), if $N > N_0$, it is possible for isopycnal displacements in the internal wave range of frequencies to force the float at the resonance frequency, ω_0. Consider for simplicity a Garrett and Munk (1975) internal wave model of the displacement spectrum $E_w(\omega)$ which for the expected case near resonance $\omega \approx \omega_0 \gg \omega_i$, ω_i the local inertial frequency, can be written as

$$E_w(\omega) = (3/2)a^2\omega_i/\omega^2, \quad (4.10)$$

where a is the canonical rms internal wave displacement, taken as 7 m from (Garrett and Munk 1975). Substitution of (4.10) into (4.9a) and (4.9b) yields

$$\Delta\omega = [4.8(a^2\omega_i(\omega_0)^2\nu^2r^2)/(R^4L^2)]^{1/5} \quad (4.11a)$$

$$Q = [0.21R^4L^2(\omega_0)^3/(\omega_i a^2\nu^2r^2)]^{1/5}. \quad (4.11b)$$

TABLE 1. Resonant frequency $\omega_0 = N_0$, and $Q_{\min}$ from (4.11a. and 4.11b) for aluminum and glass cylindrical floats deployed in mid-latitudes for relative compressibilities $s = 0.5, 0.9$.

	Aluminum		Glass	
	$s = 0.5$	$s = 0.9$	$s = 0.5$	$s = 0.9$
$\omega_0 = N_0$ (cyc hr^{-1})	5.4	2.3	13.4	5.8
$Q_{\min}$, Swallow float	4.7	3.6	10.9	5.0
$Q_{\min}$, SOFAR float	19.6	15.0	45.5	20.8

In Table 1, for the case of a long aluminum cylinder, $\alpha_f = 7.0 \times 10^{-5}$ °C^{-1}, and a long glass cylinder $\alpha_f = 10^{-5}$(°C)$^{-1}$ with $\alpha_w = 2.5 \times 10^{-4}$(°C)$^{-1}$ at 18°C, we show the minimum resonant frequency at which forcing from internal waves can occur, $\omega_0 = N_0$, i.e., $N > \omega_0 > N_0$, from (4.2). From (4.11b), $\omega_0 = N_0$ corresponds to the minimum value of Q, $Q_{\min}$, for the Garrett and Munk internal wave model with $a^2 \approx 52$ m^2. The values of Q based on the Garrett and Munk model may, in fact, be somewhat lower when $\omega_0 \approx N$, since near N internal waves can exhibit displacement values somewhat larger (Pinkel 1975; Kase and Clark 1978) than the Garrett and Munk values. However, from (4.9b) since Q is proportional to $[E_w(\omega)]^{-1/5}$ an order of magnitude increase in spectral level at N would result in only a decrease of Q by 1.6. Table 1 shows that size plays an important role in determining Q, with the larger SOFAR float exhibiting larger values of Q and thus being much more narrowband in its response to isopycnal forcing (by internal waves). The more isopycnal a float is made by increasing s, the less narrowband the resonance.

5. Observations from isopycnal floats

There is limited data available for comparison of the predicted to observed float response, particularly for the near resonance case. A developmental effort has been underway (Rossby et al. 1985; Levine et al. 1986) to increase the relative compressibility of neutrally buoyant floats, typically $s = 0.5$ to $s \geq 0.9$. In this program, an isopycnal Swallow float was deployed in the Gulf Stream (Levine et al. 1986) during May 1983, in which the float was in a meander feature where there was significant isopycnal depth change. In Fig. 5, a time series of the acoustically determined float depth is superimposed on a time series of the XBT derived 16°C isotherm depth, approximating the CTD determined $\sigma_t = 26.6$ surface tracked by the float. This isotherm showed a maximum displacement of 120 m at 1800 UTC 17 May with a float displacement $\xi_f = 80$ m, and thus a relative displacement $\xi_r = 40$ m, yielding $r = \xi_r/\xi_w = 0.33$. Using the local $N = 2$ cyc h^{-1} calculated from CTD profiles along with $s = 0.87$ obtained from laboratory measurements, and $\Omega = 3.8$ cyc h^{-1}

Unauthenticated | Downloaded 11/29/23 05:35 AM UTC

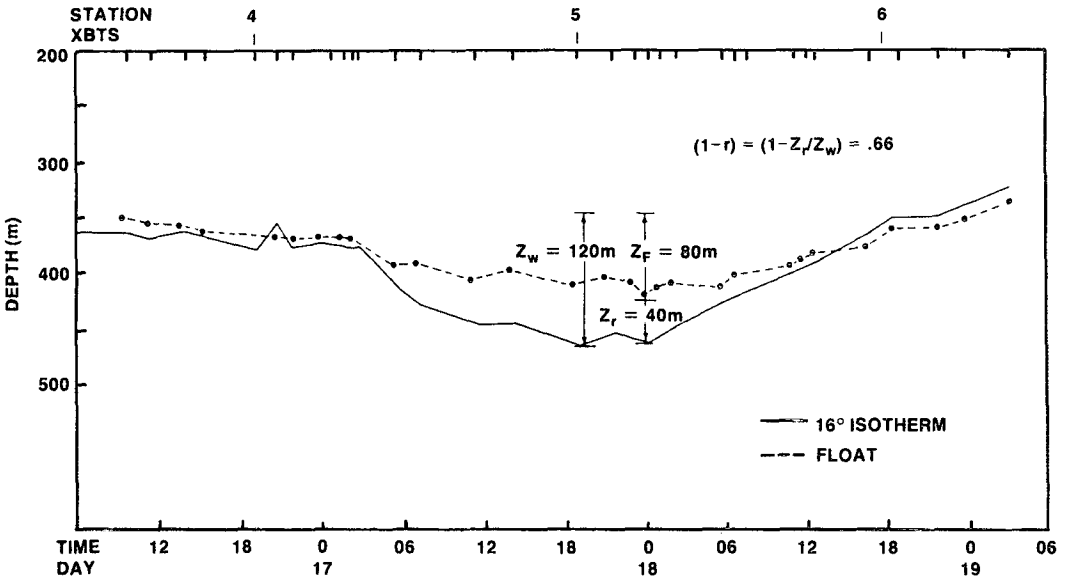

FIG. 5. Experimental determination of $(1 - r)$ from the May 1983 isopycnal Swallow float deployment in the Gulf Stream (Levine et al. 1986). XBTs and CTD stations are indicated in the figure.

in (3.3) yields a theoretical $r \approx 0.30$, close to the observed $r = 0.34$.

Data on float response at high frequencies, of order N, are difficult to obtain since floats deployed for many months typically sample only a few times per day. In a September 1986 Gulf Stream deployment, temperature and pressure were sampled every 15 minutes in a region with $N \sim 8$ cyc h^{-1}. Their time series are shown in Fig. 6. Note that there do appear to be oscillations in the pressure record with amplitudes and time scales of order internal waves. A comparison of the temperature time series with XBT data shows that the float oscillated in the depth interval corresponding to the 15°–16°C range. In Figs. 7a, b the associated pressure and temperature spectra are displayed, respectively. The pressure spectra slope is approximately −2 with frequency into the noise level at approximately 1 db^2/cyc h^{-1} as expected from the manufacturer's sensor specifications. The temperature spectra has a similar behavior, falling into the noise level at approximately 0.01(°C)^2/cyc h^{-1} which corresponds to the sensitivity of the sensor. Also, since the thermistor was located inside the float touching the glass tube, subsequent laboratory tests have shown that the time needed for the float to reach thermal equilibrium, for a $\Delta T \sim 10$°C, is greater than the 15 minute sampling rate, and so the float acts as a low-pass filter.

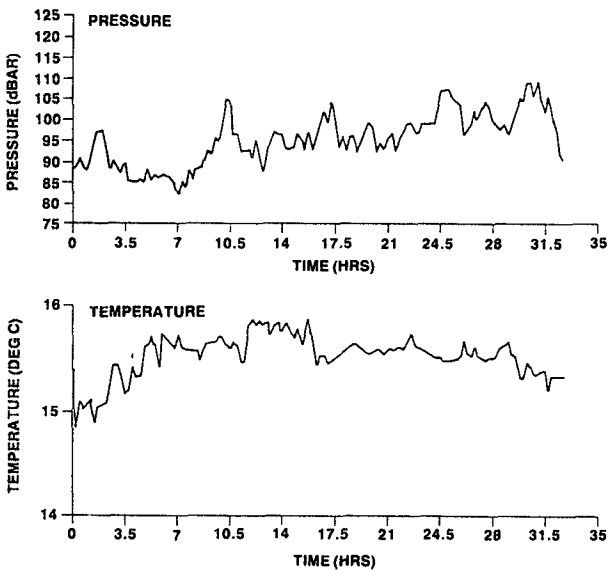

FIG. 6. Time series of isopycnal Swallow float temperature (°C) and pressure (decibars) obtained during September 1986 in the Gulf Stream region.

From section 3, if $Q \gg 1$ for frequencies $\omega < \omega_0$ for an isopycnal-like float, we would expect, in a region of uniform temperature gradient, that the temperature spectrum, ϑ_T, is related to the pressure spectrum, ϑ_P, by

$$\vartheta_T \approx [(dT/dz)^2 r^2/(1 - r)^2]\vartheta_p = B\vartheta_P, \quad (5.1)$$

where r is the response ratio, dT/dz is the temperature gradient, and B is the scaling factor:

$$B = (dT/dz)^2 r^2/(1 - r)^2 = 1.2 \times 10^{-3}(°C)^2\ m^{-2}. \quad (5.2)$$

for the observed values $r = 0.34$, and $dT/dz = 6.6 \times 10^{-2}$ °C m^{-1}. The scaled pressure spectrum, $B\vartheta_p$,

Unauthenticated | Downloaded 11/29/23 05:35 AM UTC

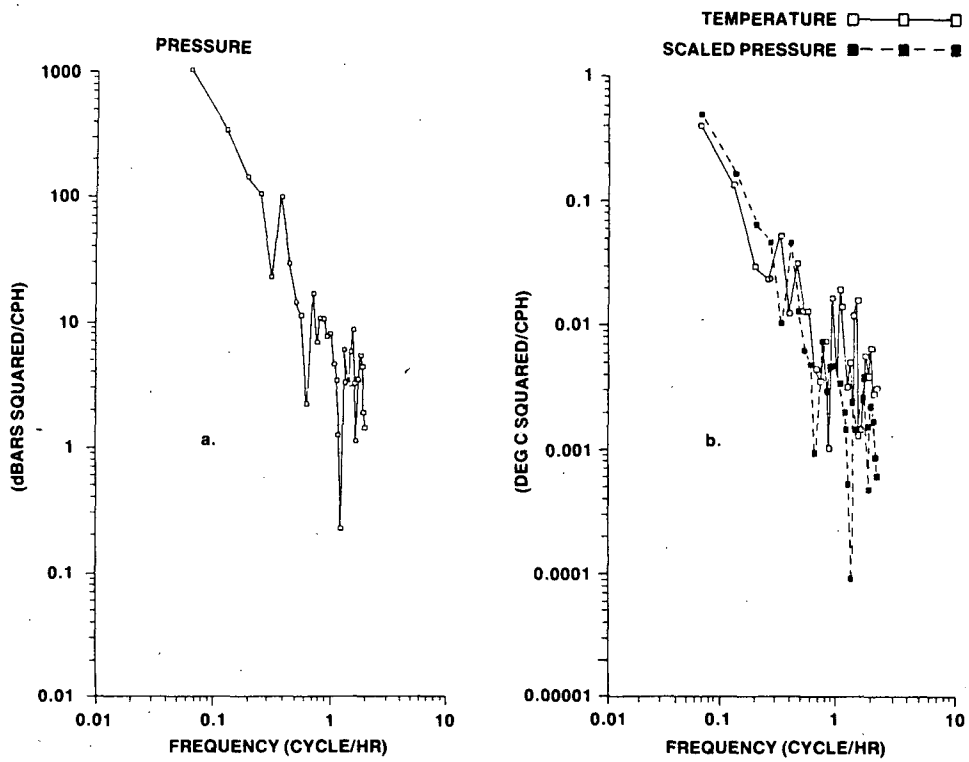

FIG. 7. (a) Float sensor pressure spectrum (db^2/cph) as a function of frequency (cph) from the Gulf Stream region deployment data in Fig. 8. (b) The scaled pressure spectrum (5.1) from (a) superimposed on the float sensor temperature spectrum ($°C^2/cph^{-1}$) as a function of frequency (cph).

shown as the dotted line in Fig. 7b, does line up reasonably well with the temperature spectrum.

For this dataset, a rough estimate of a lower bound on Q from (4.9b) can be made using the pressure power spectral estimate ϑ_p extrapolated with a -2 power law to the resonant frequency, ω_0. Using

$$E_w(\omega_0) = E_f(\omega_0)/(1 - r)^2 \approx \vartheta_P(\omega_0)/(1 - r)^2, \tag{5.3}$$

from (4.1) for $\omega_0 \approx 7.9$ cyc h^{-1}, we obtain $\vartheta_P(\omega_0) \approx 3.0 \times 10^{-2}$ $db^2/(\text{cyc } h^{-1})$ for $r = 0.34$, and float values of $R = 0.04$ m and $L = 1.32$ m yield $Q \approx 5$, supporting the assumption of narrowband resonance.

6. Summary and conclusions

The vertical response of a neutrally buoyant float to isopycnal displacements is modeled as a nonlinear, forced, damped, harmonic oscillator, following the approach of Voorhis (1971). After initial deployment and after equilibrium is reached, the response of a float to an isopycnal displacement from its initial equilibrium position can be characterized by a near equilibrium response regime and a near resonance response regime. The boundary between these two frequency regimes is given by $\omega_0 - \Delta\omega$, provided $\Delta\omega \ll \omega_0$.

For the near equilibrium regime, float response is determined by the float and water material properties, i.e., γ_f, γ_w, α_f, α_w and N. Note that $\mathcal{N}$, the normalized frequency given by (3.4), is proportional to $(1 - \alpha_f/\alpha_w)$ and that as $\alpha_f \to \alpha_w$, $\mathcal{N} \to 0$. Thus increasing α_f to α_w has the same effect as decreasing N. For the case of long cylinders, body size and shape can be ignored in the near equilibrium regime. Near isopycnal behavior occurs for $s \approx 1 \pm \delta s$, $\delta s \ll 1$. However, in situ variation in s can result from effects such as variability in γ_w, buoyancy effects of bubbles adhering to surfaces, and creep in the float body. The requirement of stable equilibrium imposes a constraint on δs (Figs. 2a, b) that increases with decreasing N. Thus, it is more difficult to achieve near-isopycnal behavior in low N regions. The response ratio, r, calculated from an isopycnal float deployment in a Gulf Stream meander, was close to the theoretical value estimated from float and seawater material properties.

For the near resonance regime, vertical motion depends on drag, in addition to the material properties of the float and seawater. The normalized bandwidth, $Q = \omega_0/\Delta\omega$, is used as a measure of the sharpness of the resonant response. For typical cylindrical floats used in oceanography, Swallow and SOFAR, float response from vertical forcing by Garrett and Munk (1975) in-

Unauthenticated | Downloaded 11/29/23 05:35 AM UTC

ternal waves (4.11b) results in $Q > 1$ and typically $Q \gg 1$. For a Swallow float deployment in the Gulf Stream region we obtained a calculated $Q \approx 5$.

Since float response is typically narrowband about a resonant frequency which is of order or larger than the local buoyancy frequency, floats presently being used in larger scale studies could be adapted to measure internal waves. In addition, time series of temperature and pressure, the usual data currently sampled by floats, can be used in (5.2) along with knowledge of material properties of the float to determine dT/dz, provided either dS/dz makes negligible contribution to N or the T–S relation is known. Note that the resonant frequency, given by (4.1), is a function of the local buoyancy frequency and float material properties. Thus, in regions where salinity gradient is important and it would not be possible to use (5.2) to estimate N, it may be possible to estimate N from the location of spectral peaks in pressure or temperature provided there is sufficient vertical forcing at ω_0 and $Q \gg 1$.

Acknowledgments. The authors wish to thank Naval Underwater Systems Center IR/IED program and the Office of Naval Research Code 1125 AR for their support of this research.

REFERENCES

Batchelor, G. K., 1967: *An Introduction to Fluid Dynamics.* Cambridge University Press, 1–615.

Cairns, J. L., 1975: Internal wave measurements from a midwater float. *J. Geophys. Res.*, **80,** 299–306.

——, and G. O. Williams, 1976: Internal wave observations from a mid-water float, 2. *J. Geophys. Res.*, **81,** 1943–1950.

——, W. Munk and C. Winant, 1979: On the dynamics of neutrally buoyant capsules: An experimental drop in Lake Tahoe. *Deep-Sea Res.*, **26a,** 369–381.

Garrett, C. J. R., and W. H. Munk, 1975: Space-time scales of internal waves: A progress report. *J. Geophys. Res.*, **89,** 291–297.

Gascard, J. C., and R. A. Clark, 1983: The formation of Labrador Sea water. Part II: Mesoscale and smaller processes. *J. Phys. Oceanogr.*, **13,** 1779–1797.

Hitchcock, G., E. J. Lessard, D. Dorson, J. Fontaine and T. Rossby, 1989: The IFF: The Isopycnal Float Fluorometer. *J. Oceanic Atmos. Technol.*, **6,** 19–25.

Kase, R. H., and R. A. Clarke, 1979: High frequency internal waves in the upper thermocline during GATE. *Deep-Sea Res.*, **25,** 227–232.

Kinsler, L. E., A. R. Frey, A. B. Coppens and J. V. Sanders, 1982: *Fundamentals of Acoustics.* Wiley and Sons, 1–480.

Larsen, L., 1969: Oscillations of a neutrally buoyant sphere in a stratified fluid. *Deep-Sea Res.*, **16,** 1–36.

Levine, E. R., D. N. Connors, P. C. Cornillon and H. T. Rossby, 1986: Gulf Stream kinematics along an isopycnal float trajectory. *J. Phys. Oceanogr.*, **13,** 1317–1328.

Manley, T. O., J.-C. Gascard and W. B. Owens, 1989: The Polar Floats Program. *IEEE J. Oceanic Engineering,* **14,** 186–194.

Morison, J., and R. Anderson, 1985: Data report, profiles of temperature, salinity, and velocity made with the Arctic profiling system during Fram III. APL Tech Memo 1-85, University of Washington, Polar Science Center,

Pinkel, R., 1975: Upper ocean internal wave observations from *FLIP. J. Geophys. Res.*, **80,** 3892–3910.

Pochapsky, T. E., 1963: Measurement of small-scale oceanic motions observed with neutrally buoyant floats. *Tellus,* **15,** 353–362.

Price, J., and H. T. Rossby, 1982: Observations of a barotropic planetary wave in the Western North Atlantic. *J. Mar. Res.*, **40**(Suppl.), 543–548.

Rossby, H. T., A. D. Voorhis and D. Webb, 1975: A quasi-Lagrangian study of mid-ocean variability using long range SOFAR floats. *J. Mar. Res.*, **33,** 355–382.

——, E. R. Levine and D. N. Connors, 1985a: The Isopycnal Swallow float—a simple device for tracking water parcels in the Gulf Stream. Progress in Oceanography. 14, *Essays on Oceanography, a Tribute to John Swallow.* J. Crease, W. J. Gould and P. M. Saunders, Eds., Pergamon, 511–525.

——, A. S. Bower and P. T. Shaw, 1985b: Particle pathways in the Gulf Stream. *Bull. Amer. Meteor. Soc.,* **66,** 1106–1110.

——, D. Dorson and J. Fontaine, 1986: The RAFOS system. *J. Atmos. Oceanic Technol.*, **3,** 672–679.

Schlicting, H., 1968: *Boundary Layer Theory.* McGraw Hill, 747 pp.

Swallow, J. C., 1955: A neutral-buoyancy float for measuring deep currents. *Deep-Sea Res.*, **3,** 74–81.

Voorhis, A. D., 1968: Measurements of vertical motion and the partition of energy in the New England Slope Water. *Deep-Sea Res.*, **15,** 599–608.

——, 1971: Response characteristics of neutrally buoyant floats. Woods Hole Oceanogr. Publ. 71-73, 1–56.

Weller, R. A., J. P. Dean, J. Marra, J. F. Price, E. A. Francis and D. C. Boardman, 1985: Three dimensional flow in the upper ocean. *Science,* **227,** 1552–1556.

Williams, A. J., III, C. H. Converse and J. W. Nicholson, 1987: Richardson Number Float. *Current Practices and New Technology in Ocean Engineering,* OED Vol. 12, G. K. Wolf, Ed., Amer. Soc. Mech. Eng., 25–29.

Unauthenticated | Downloaded 11/29/23 05:35 AM UTC